EasyChair Preprint

№ 15350

Experimental Study of an Evaporative Condensation Refrigerant Pump Heat Pipe Air-Conditioning Unit Based on a Microchannel Heat Exchanger

Junjie Chu, Xiang Huang, Hongxu Chu, Liu Yang, Ying Wang, Xing Tang and Tianlei Shen

November 1, 2024

Title: Experimental study of an evaporative condensation refrigerant pump heat pipe air-conditioning unit based on a microchannel heat exchanger

junjie chu[1,2], xiang huang[1], hongxu chu[3], liu yang[1] ying wang[4] xing tang[5] jinxing tian[1]

[1] School of Urban Planning and Municipal Engineering, Xi'an Polytechnic University, chujunjie2010@foxmail.com
[2]State Key Laboratory of Building Safety and Built Environment
[3]College of Environment and Chemical Engineering, Yan shan University
[4]School of Building Services Science and Engineering, Xi'an University of Architecture and Technology,
[5] LUE-ON (Jiangsu) Environmental System Co., Ltd., Tai xing

Abstract: A new evaporative condensation refrigerant pump heat pipe air-conditioning unit based on a microchannel heat pipe heat exchanger is proposed. Performance experiments are conducted of the unit, and the experimental results show that the cooling capacity of the unit in the dry, wet, and mixed modes can reach 112.1, 105.8, and 115.4 kW, respectively, the optimal airflow ratio of the secondary/primary airflow is 2.2, 1.8, and 1.8, respectively, and the EER decreases with increasing airflow ratio. With increasing dry- and wet-bulb temperatures of the secondary-side inlet air, the cooling capacity and energy efficiency ratio of the unit decrease, and the energy efficiency ratio in the wet mode is higher than that in the dry mode, which can prolong the operating hours of the wet mode within the operating temperature range of the dry mode and improve the energy efficiency of the unit. A new calculation method for the refrigerant charge is proposed, and the optimal refrigerant charge is 32 kg based on the experimental results, which agrees with the theoretical calculation results

Keywords: Evaporative cooling; Evaporative condensation; Refrigerant pump system; Heat pipe; Refrigerant charging

1. INTRODUCTION

Over the past five years, China's data center energy consumption has rapidly increased at a rate of more than 10% per year, and the power consumption of data centers in 2021 was approximately 94 billion kW-h (Insight 2021, YEAR:2021 page 4), accounting for 2.7% of the total electricity consumption of society as a whole. IT equipment at data centers accounts for approximately 45% of the total energy consumption, refrigeration and air-conditioning systems account for approximately 40% of the total energy consumption, power supply and distribution, and other facilities account for approximately 15% of the total energy consumption. The use of refrigeration and air-conditioning systems is the main reason for the current high data center energy consumption, which can be resolved by reducing the energy consumption of air-conditioning systems at data centers and improving the overall efficiency of these systems. The temperature at data centers, after absorbing the heat produced by chips from the air, usually ranges from 35~38 ℃, and during most of the year, the outdoor environment exhibits a temperature difference of 10~25 ℃ because the use of natural cold sources involves a large development space. In recent years, evaporative cooling technology, liquid cooling technology, and refrigerant pump heat pipe technology have gradually been adopted. Heat pipe technology fully utilizes the principle of heat conduction, provides the advantages of rapid heat transfer and low heat loss(Jiang L, Yong T, Wei Z, et al, YEAR:2014 page 292-301), and can be combined with microchannel heat exchangers and evaporative condensation and other technologies to effectively improve the heat transfer efficiency of heat pipe systems to extend the use of natural cold sources over time.

Liu Chenpeng (Liu C，Chen Y，Feng D,et al, YEAR:2022 page 210) et al. applied a large-area low-temperature loop heat pipe in heat dissipation of an optical telescope, which demonstrated the practical feasibility of applying loop heat pipes on a large scale in engineering. By applying a heat pipe system in the field of data center engineering, GY Ma (Ma G Y，Wei C C，Zhang S，et al, YEAR:2015 page 439-445) et al. investigated the operational performance of a refrigerant pump-driven loop heat pipe at a small data center, and the results showed that the EER varied with the change in the outdoor temperature, while the refrigerant pump heat pipe system could satisfy the heat load at an outdoor temperature lower than 15 °C, realizing a minimum energy-saving effect of 36.57%. Jiankai Dong (A J D，A Y L，B S D，et al, YEAR:2017 page 560-568) et al. studied a refrigeration system combining a refrigerant pump refrigerant two-phase delivery cycle and vapor compression, which significantly improved the energy efficiency relative to the traditional system but was greatly affected by the ambient outdoor temperature; at ambient temperatures of 3.2 and 12.0 °C, 80% and 50% of the design value, respectively, could be obtained. Yan Gang (Yan G, Feng Y, Peng L, YEAR:2022 page 11-18) coupled a vapor compression refrigeration system with a refrigerant pump refrigeration system and investigated the effect of various switching temperature points between different operating conditions on the overall system energy efficiency, with a suitable changeover temperature of -5 °C. Shuailing Liu (Shuailing L, Guoyuan M, Xiaoya J, et al, YEAR:2022 page 118066) et al. proposed a loop heat pipe heat recovery system driven by a refrigerant pump and investigated the effect of three operating modes in winter and summer, with suitable changeover temperatures of -4 and -5 °C, respectively. The heat transfer characteristics in the three operating modes in winter and summer were investigated. The results showed that the pump-driven loop heat pipe mode attained the highest efficiency under year-round conditions. F Chen (Chen F, Zhou X, Liao S, YEAR:2022 page 1-20) compared a refrigerant pump air conditioner, a chiller unit, and a gravity heat pipe dual-cycle air conditioner and found that the annual operating time of the gravity heat pipe dual-cycle air conditioner was 50.8% longer than that of the refrigerant pump air conditioner. The gravity heat pipe dual-cycle air conditioner could achieve energy savings of approximately 34% relative to the chiller unit.

Refrigerant pumps are used as power drive devices in separated heat pipe systems, which can overcome the limitations of heat pipe system arrangement sites and application scenarios. Shuailing Liu et al. proposed a loop heat pipe heat recovery system driven by refrigerant pumps and investigated the heat transfer characteristics under three operating modes in winter and summer. The results showed that the pump-driven loop heat pipe mode provided the highest temperature efficiency under year-round conditions(Shuailing L，Guoyuan M，Xiaoya J，et al, YEAR:2022 page 207). The heat exchanger of the refrigeration system uses a microchannel heat exchanger, which provides the advantages of high heat transfer efficiency and low charge work mass. MM Ohadi et al. applied a new microchannel-powered heat pipe refrigeration system at a data center and evaluated its performance via a comparison with the traditional compressor system, and the experimental results showed that it could greatly reduce the power consumption of the system(Ohadi M M，Dessiatoun S V，Choo K，et al, YEAR:2012 page 58-63). Aibo Wei et al. used CFD simulation software to simulate the heat transfer process of an Ω-shaped microchannel heat exchanger used in gravity-separated heat pipe systems. The use of a microchannel heat exchanger can facilitate large-distance heat transfer by the heat pipe system at the cost of a very small temperature difference (Wei A，Ren X，Lin S，et al, YEAR:2020 page 120488). A heat pipe system combined with evaporative condensation technology fully extends the utilization of natural cooling sources. Z Han proposed a combined air-conditioning system in which the air velocity of the condenser and the operating frequency of the refrigerant pump could be adjusted, and it was found that evaporative condensation effectively extended the operating range of the heat pipe mode and increased the upper limit of the outdoor temperature from 8 to 15 °C (Han Z , Xue D , Wei H , et al, YEAR:2021 page 177).

MaYuezheng(Yue zheng M , Shu xue X , Guo yuan M ,et al, YEAR:2016 page 1-5) examined a refrigerant pump-driven evaporative condensation composite refrigeration system, and the results showed that the system energy efficiency ratio

was the highest at an outdoor temperature of 15℃ and an air velocity of 1 m/s, and the optimal temperature switching point between the two operating modes was experimentally obtained. LinYucong (Lin Yucong, Liu Jinping, Xu Xiongwen ,et al, YEAR:2020 page 83-88)designed and conducted experiments with a refrigerant pump pressurized air-conditioning system, and the results showed that the use of a refrigerant pump pressurized air-conditioning system could achieve 100% refrigeration at working temperatures ranging from -5 to 25 ℃ to meet the operating requirements of computer room air conditioning. Xue Lianzheng(Xue Lianzheng, Ma Guoyuan, Zhou Feng, et al, YEAR:2019 page 1-9)applied an air pump-driven refrigeration air-conditioning unit at a data center in Beijing. The experiment revealed that with increasing indoor/outdoor temperature difference, the unit heat transfer volume increased, the air pump operating power decreased, and the annual energy saving rate reached 25.78%. BaiKaiyang et al. (Bai Kaiyang, Ma Guoyuan, Zhou Feng , et al, YEAR:2016 page 109-115)coupled a plate heat exchanger with mechanical refrigeration, yielding a refrigerant pump-driven circuit heat pipe, which could realize three operating modes, and the highest energy-saving rate of up to 49.4% was attained in different regions of China. Liu Zhenyu (Liu Zhenyu, Huang Xiang, Chang Jianpei , et al, YEAR:2020 page 6)designed an experimental prototype by combining evaporative condensation, evaporative cooling and mechanical refrigeration technologies and conducted experiments and energy consumption analysis tests of each functional section, proving that the annual power saving rate of this unit could reach 51.4%.

Summarizing the above literature, we can find that there have been explorations and engineering applications of refrigerant pump heat pipe air-conditioning systems in the field of data centers; however, there are still problems that must be solved, such as an excessive volume, low efficiency, and the determination of the optimal refrigerant charge. For this reason, we proposed a new evaporative condensation and microchannel refrigerant pump heat pipe coupled refrigeration system for data centers, which improved the heat transfer performance of the heat pipe through the use of a microchannel heat exchanger, and we combined it with high-efficiency evaporative condensation cooling technology to improve the heat transfer efficiency of the unit. This approach can not only extend the use of natural cooling sources but also reduce the system footprint space through the integration of these two systems. In this paper, we mainly analyzed the advantages of the power heat pipe system using a microchannel heat exchanger considering the evaporative condensation principle. We experimentally assessed the performance of the microchannel heat pipe evaporative cooling air-conditioning unit, thereby considering three unit operating modes as well as the air volume ratio and cooling capacity, and we obtained the relationship between the energy efficiency ratio, optimal refrigerant charge and refrigeration capacity of the heat pipe system via the experiments. We summarized the challenges in the design and test process and proposed a new method for calculating the refrigerant charge of the refrigerant pump heat pipe system

2. INTRODUCTION OF THE UNIT

The unit is designed with a rated cooling capacity of 120 kW, of which the mechanical refrigeration system provides a make-up capacity of 60 kW. It adopts a one-piece design, including two parts: an indoor side and an outdoor side. The secondary air (working air) of the outdoor side is filtered through the air inlet before entry, and after enthalpy reduction in the wet film packing section, the air flows through the microchannel heat pipe condenser and the mechanical refrigeration condenser sequentially to remove heat. Finally, the air is discharged to the outdoors through the air outlet. The indoor-side primary air (output air) flows through the air inlet into the microchannel heat pipe evaporator, mechanical refrigeration evaporator and other wet cooling system sections and then through the air supply opening into the room to complete the cycle. Regarding organic combination of the heat pipe refrigeration system, mechanical refrigeration system, and wet film packing system, the specific principle and structure of the unit are shown in Figure 1.

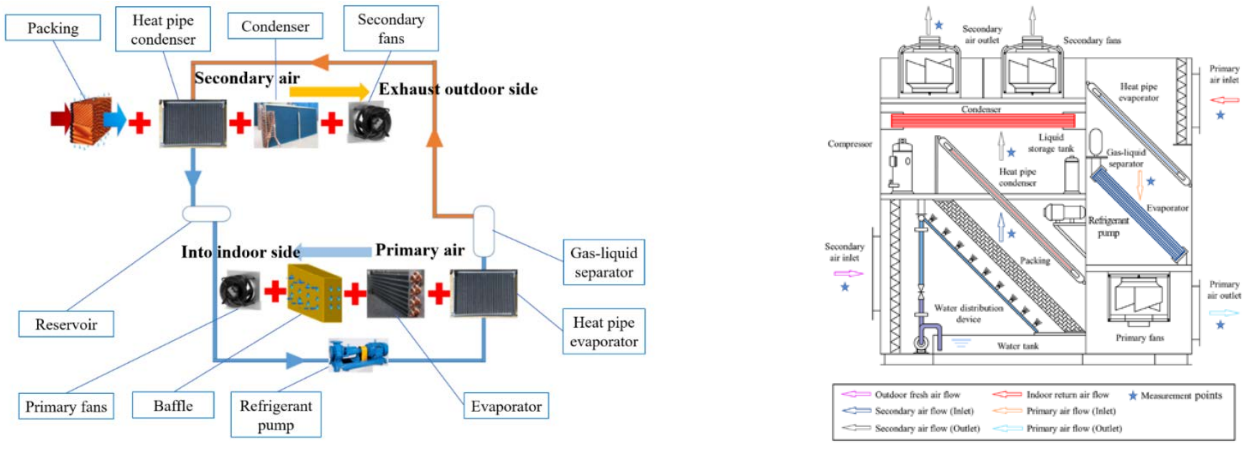

(a) Schematic diagram *(b) Structure diagram*

Figure. 1. Principle and structure diagram of the evaporation and condensation microchannel separation heat pipe unit

When the dry-bulb temperature of the outdoor air (T_{db}) is lower than 14 ℃, the unit is operated in the dry mode, the refrigerant pump overcomes the resistance of the heat pipe refrigeration system network to ensure the continuous

operation of the refrigeration system, the spraying system exhibits the closed state, the secondary air flows through the heat pipe condenser to remove heat from the data center, and the heat pipe refrigeration system bears the full load of the data center. At this time, the factor that directly affects the condensing effect of the unit is the dry-bulb temperature of the outdoor air. When the outdoor air dry-bulb temperature (T_{db}) is higher than 14 ℃ and the wet-bulb temperature (T_{wb}) is lower than 14 ℃, the unit is operated in the wet mode, the sprinkler system starts to work, the outdoor secondary air in the secondary channel first flows through the packing section and water to realize full heat and humidity exchange under enthalpic cooling, and the heat absorbed by the heat pipe condenser is discharged to the outdoors. At this time, the cooling effect of the unit is directly determined by the outdoor air wet-bulb temperature. When the outdoor air wet-bulb temperature (T_{wb}) is higher than 14 ℃, the heat pipe cooling system removes heat from the data center. When the wet-bulb temperature of the outdoor air (T_{wb}) is higher than 14 °C, the use of a natural cold source cannot meet the cooling demand of the data center, and it is necessary to employ mechanical refrigeration to compensate for the cold source. The enthalpy and humidity diagram of the air treatment process is shown in Figure 2.

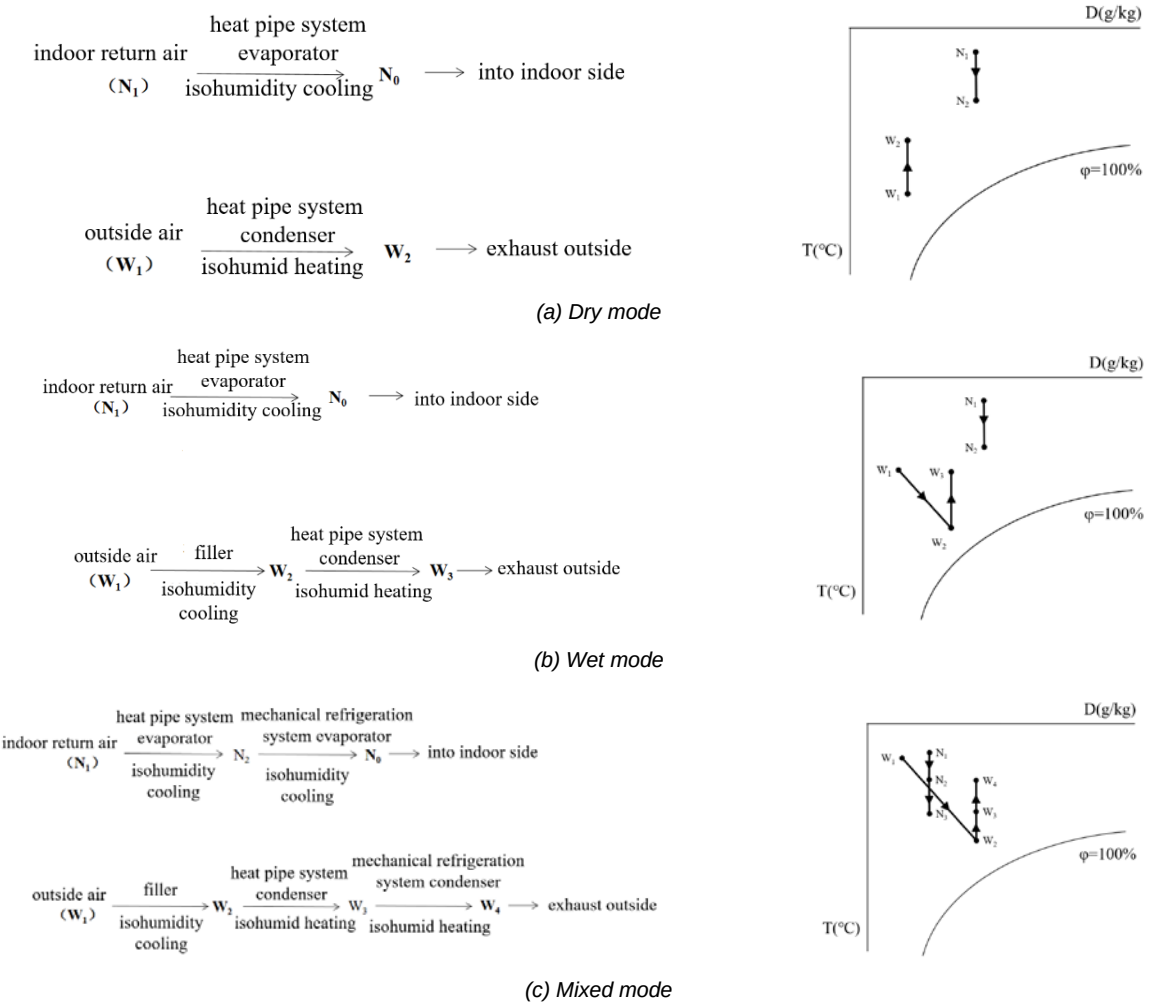

(a) Dry mode

(b) Wet mode

(c) Mixed mode

Figure. 2 Working process of the secondary/primary air in three operating modes of the unit

The starting and stopping conditions of the equipment corresponding to the three operating modes of the unit are listed in Table 1..

Table 1: Unit operating modes and equipment startup and shutdown conditions

Mode	Ambient air parameters	Fan	Water Pump	Refrigerant pump	Compressor
dry mode	Tdb≤14 °C	ON	OFF	ON	OFF
wet mode	Tdb>14 °C, Twb≤14 °C	ON	ON	ON	OFF
mixed mode	Twb>14 °C	ON	ON	ON	ON

3. DISCUSSION OF THE EXPERIMENTAL RESULTS

3.1. Experimental conditions and test contents

The proposed evaporative condensation refrigerant pump heat pipe air-conditioning unit was evaluated at an enthalpy difference laboratory in Jiangsu Province, China. The refrigeration system of the unit consists of a refrigerant pump heat pipe system and a mechanical refrigeration system, along with a spray system and wet film packing section. The shape and internal structure of the experimental prototype are shown in Figures 3 and 4, respectively.

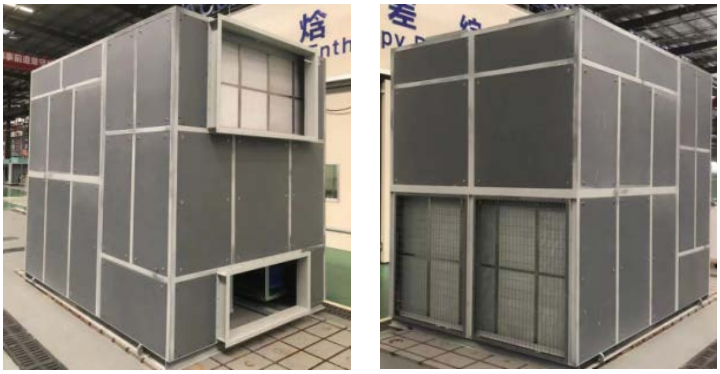

Figure. 3. Outline drawing of the air-conditioning unit

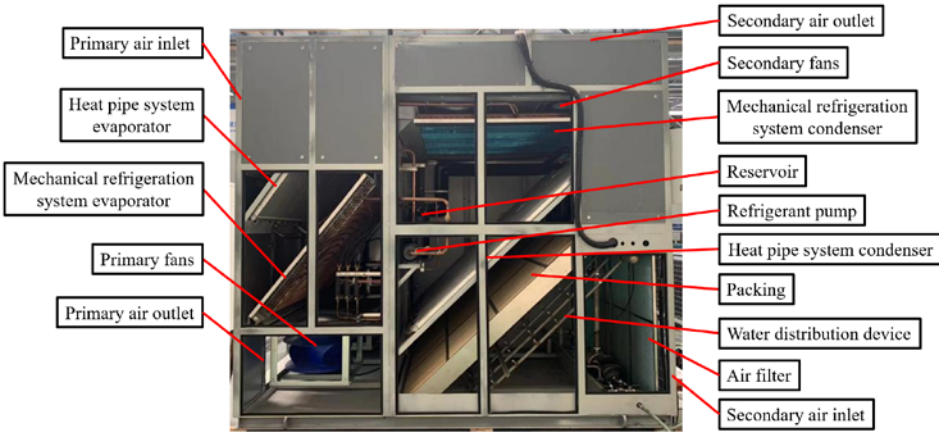

Figure. 4. Physical diagram of the unit

Referring to the Data Center Design Code (GB 50174-2017, YEAR:2017 page 32-40) and Data Center Evaporative Cooling Air-Conditioning Equipment (T/DZJN 27—2021, YEAR:2021 page 7-12) standards for data center air-conditioning unit experimental working conditions, the experimental working conditions for each operating mode were determined, as listed in Table 2.

Table 2: Unit experimental conditions

Mode	Outdoor side Air inlet state				Indoor side Air inlet state			
	dry bulb (℃)	wet bulb (℃)	dew point (℃)	air volume (m^3/h)	dry bulb (℃)	wet bulb (℃)	dew point (℃)	air volume (m^3/h)
dry mode	35.0	19.5	10.6	30000	38.0	22	Not lower than the tap water temperature	66000
wet mode	17	13	10		38.0	22	Not lower than the tap water temperature	
mixed mode	14	/	/		38.0	22	/	

In the case that the indoor and outdoor sides reach the set working conditions and the unit is stably operated, the experimental data are recorded by the experimental bench at 1-minute intervals, each working condition is maintained for 30 minutes, and the arrangement of the primary and secondary sides in the field experiments is shown in Figure 5.

(a) Indoor side (b) Outdoor side

Figure. 5. Unit test site

3.2. Uncertainty analysis of the experimental data

The physical quantities used in the experiments included measured and calculated values. The measured and calculated values were obtained directly from the measuring instruments and relevant calculation equations, respectively. The uncertainty in the experimental data could be classified as absolute or relative. The directly measured uncertainty value x could be expressed as follows:

Equation 1:

$$x = x_{meas} \pm \delta x$$

It was assumed that the indirectly calculated quantity (R) was a function of several independent measurements, and the number of independent measurements was n. The function could be expressed as follows:

Equation 2:

$$R = f\left(x_1, x_2, \cdots, x_n\right) \pm \delta R$$

Equation (3) could be used to calculate the experimental uncertainty indirectly:

Equation 3:

$$\frac{\delta R}{R} = \sqrt{\sum_{i=1}^{n}\left(\frac{\partial R}{\partial x_1}\delta x_1\right)^2}$$

According to the calculations, the uncertainties in the unit cooling capacity and EER ranged from 1.198% to 1.353% and f rom 1.589% to 1.727%, respectively, under the given operating conditions.

3.3. Experiment of the optimal airflow ratio

The unit is run in the above three operating modes in the secondary/primary air volume ratio experiment. The primary side air volume remains unchanged, and the secondary-side air inlet air velocity is measured at 10 points (the secondary-side air inlet velocity is measured at each point, and the weighted average is calculated according to the cross-sectional area of the duct to obtain the secondary-side air inlet velocity). The arrangement of the measurement points is shown in Figure 6, and the corresponding air velocity and fan input percentage under the different air volume ratios are provided in Table 3.

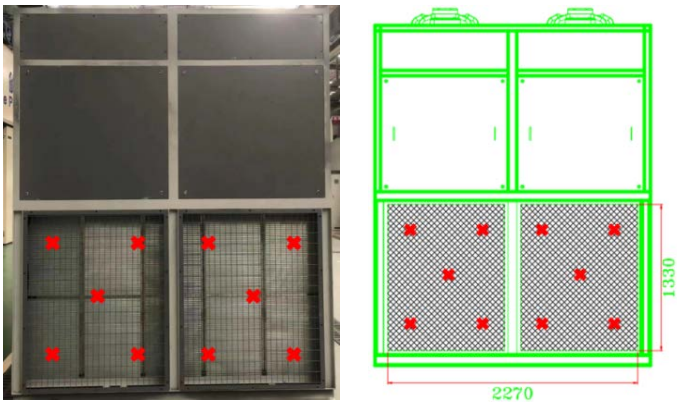

Figure. 6. Layout of the air volume measurement points

Table 3: Wind speed and fan input ratio under the different air volume ratios

Air volume ratio	Secondary air volume (m³/h)	Secondary air velocity (m/s)	Percentage of the fan input (%)
0.8	24000	2.2	40
1	30000	2.8	55
1.2	36000	3.3	63
1.4	42000	3.9	70
1.6	48000	4.4	82
1.8	54000	5.0	88
2	60000	5.5	90
2.2	66000	6.1	100

The secondary/primary airflow ratio in the dry mode ranges from 0.8 to 2.2, and the results are shown in Figure 7, where the cooling capacity of the unit increases with increasing airflow ratio, and the primary-side air outlet temperature decreases with increasing airflow ratio. At a secondary/primary airflow ratio of 2.2, the cooling capacity reaches the maximum value of 112.1 kW, and the air outlet temperature reaches the minimum value of 22.3℃. The refrigeration capacity of the unit in the dry mode is positively related to the secondary/primary airflow, the refrigeration capacity of the heat pipe system increases with increasing airflow on the secondary side, and the optimal airflow ratio in the dry mode is 2.2.

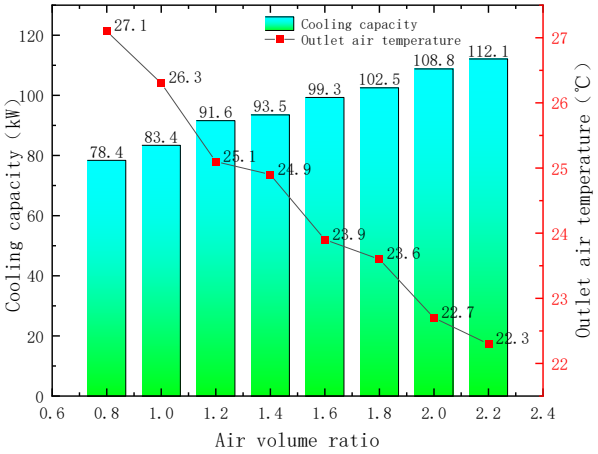

.Figure. 7 Different air volume ratios in the unit dry mode

The airflow ratio experiment of the unit was conducted under the working conditions of the wet mode. The secondary/primary airflow ratio ranged from 0.8 to 2.2, and the results are shown in Figure 8. The airflow ratio increased from 0.8 to 1.8 in the wet mode, the cooling capacity gradually increased, the primary-side air outlet temperature gradually decreased, the cooling capacity reached the maximum value of 105.8 kW at a secondary/primary airflow ratio of 1.8, the air outlet temperature reached the minimum value of 23.9℃, the cooling capacity increased from 1.8 to 2.2 at a secondary/primary airflow ratio of 1.8, and the air outlet temperature gradually decreased. When the secondary/primary airflow ratio was increased from 1.8 to 2.2, the cooling capacity gradually decreased, the air temperature on the primary side gradually decreased, and the optimal airflow ratio was 1.8.

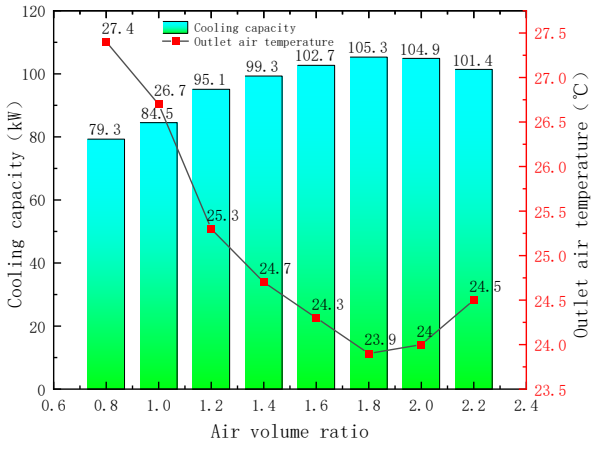

Figure. 8 Different air volume ratios in the unit wet mode

The airflow ratio experiment of the unit was conducted in the mixed mode, and the results are shown in Figure 9. When the secondary/primary airflow ratio was increased from 0.8 to 1.8, the cooling capacity gradually increased, the air outlet temperature gradually decreased, the cooling capacity reached the maximum value of 115.4 kW at a secondary/primary airflow ratio of 1.8, the air outlet temperature reached the minimum value of 22.6 °C, the cooling capacity gradually decreased at a secondary/primary airflow ratio ranging from 1.8 to 2.2, and the optimal airflow ratio was 1.8. When the secondary/first airflow ratio was increased from 1.8 to 2.2, the cooling capacity gradually decreased, the air temperature on the primary side gradually increased, and the optimal airflow ratio was 1.8.

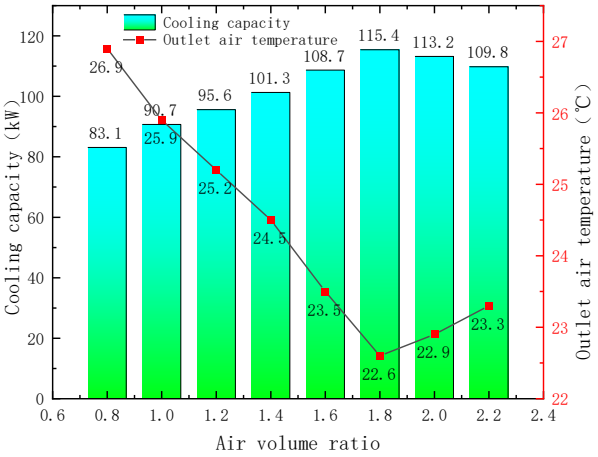

Figure. 9 Unit supplementary cooling mode for the different air volume ratios

In the three operating modes, the different secondary/primary air volume ratios resulted in unit energy efficiency ratio (EER) changes, as shown in Figure 10. The EER comparison results indicated the following order: dry mode > wet mode > mixed mode. The reason is that the wet mode started after the pump was activated, while the mixed mode started after the compressor was turned on. Moreover, the input power increased with increasing cooling capacity, but the input power increased more notably than the cooling capacity. Therefore, the unit EER decreased.

As the secondary/primary air volume ratio is gradually increased, the unit EER decreases. The reason for this phenomenon is that the air on the secondary side of the unit must flow through the filter, wet film packing, heat pipe microchannel heat exchanger, and mechanical refrigeration condenser in sequence, the overall wind resistance is high, the fan input power increases, and the fan input power more notably increases than the cooling capacity. It can be concluded that the unit with the highest cooling capacity and EER does not necessarily provide the optimal energy efficiency ratio. The secondary side achieves a better energy efficiency-related performance in the low-airflow state than in the high-airflow state, which can ensure that the secondary-side fan of the unit is operated in the low-airflow state when the data center load or the outdoor temperature is lower, thus ensuring a higher EER; at the same time, it is necessary to further optimize the structure of the secondary side of the unit to reduce the wind resistance and further enhance the EER.

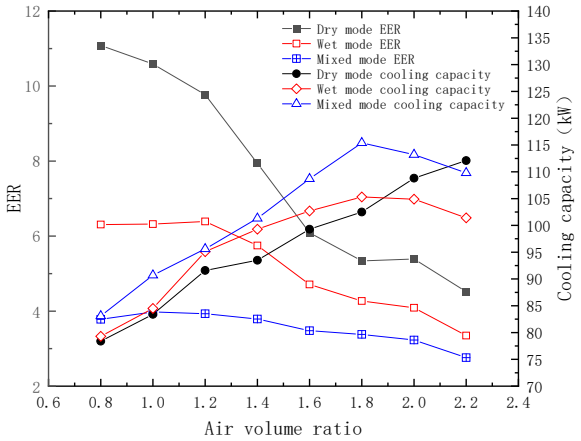

Figure. 10 EER and cooling capacity of the unit for the different air volume ratios

3.4. Inlet air temperature test

At the optimal secondary/primary airflow ratios of 2.2 and 1.8 in the dry and wet modes, respectively, the effect of the secondary-side inlet air temperature on the cooling capacity of the unit is investigated. When the unit is operated in the dry mode, since only the refrigerant pump heat pipe system is turned on, the influence of the wet-bulb temperature of the incoming air on the secondary side on the cooling capacity can be ignored, and only the influence of dry-bulb temperature change on the cooling capacity is considered. As shown in Figure 11, when the dry-bulb temperature increases from 12 to 20 °C, the cooling capacity of the unit decreases from 133.9 to 63.6 kW, and the primary-side air outlet temperature gradually increases from 19.2 to 29.1 °C. With increasing secondary-side air inlet temperature, the cooling capacity of the unit decreases from 133.9 to 63.6 kW. As the air inlet temperature on the secondary side is increased, the cooling capacity of the unit gradually decreases, and the outlet temperature on the primary side gradually increases.

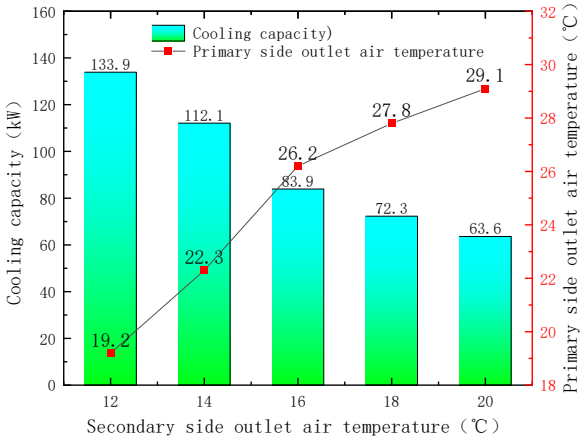

Figure. 11. Influence of the secondary-side inlet air temperature on the unit cooling capacity in the dry mode

When the unit is operated in the wet mode, the pump is turned on, direct evaporative cooling is utilized to reduce the inlet air temperature on the secondary air side, and the effects of both the outdoor air dry- and wet-bulb temperatures should be accounted for. The experimental results are shown in Figure 12. When the outdoor air dry/wet-bulb temperature increases from 12.0 °C/8.3 °C to 20.0 °C/15.4 °C, the inlet air temperature in front of the microchannel heat exchanger on the secondary air side increases from 9.3 to 16.6 °C, the cooling capacity of the unit decreases from 139.6 to 76.3 kW, and the outlet air temperature on the primary air side gradually increases from 18.4 to 27.3 °C. As the dry bulb/wet-bulb temperature on the secondary air side is increased, the cooling capacity of the unit gradually decreases, and the air outlet temperature on the primary side gradually increases.

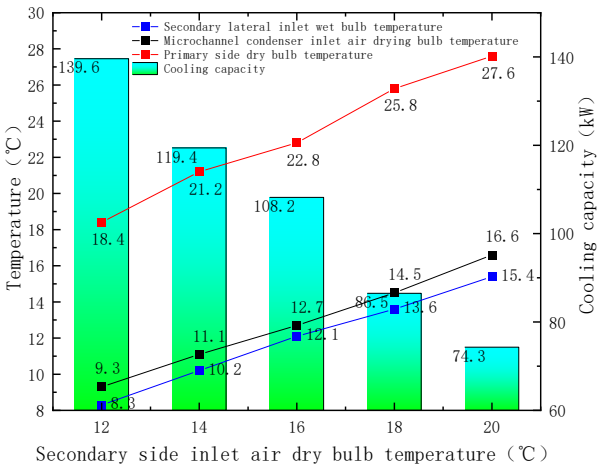

Figure. 12 Influence of the secondary-side inlet air temperature on unit cooling capacity in the wet mode

It can be concluded that the main influencing factor of the cooling capacity of the unit in the dry mode is the dry-bulb temperature of the air on the secondary side; the lower the dry-bulb temperature is, the higher the cooling capacity. The

main influencing factor of the cooling capacity of the unit in the wet mode is the wet-bulb temperature of the air on the secondary side; the lower the wet-bulb temperature is, the higher the cooling capacity of the unit. Under the same outdoor temperature change conditions, the cooling capacity in the wet mode is better than that in the dry mode, and in actual operation, it can be adjusted according to the different load conditions and the operating mode. In areas with a sufficient water supply, when the outdoor dry-bulb temperature is 10-14 ℃, the operating hours of the wet mode can be extended to adapt to the load demand of the data center.

The dry and wet modes each yield different optimal air volume ratios, the fan input power on the secondary side differs, the wet mode depends on the start of pump operation, and the input power also increases. Hence, we must explore the wet and dry mode energy efficiency ratio differences with the change in outdoor ambient temperature.

The dry-bulb temperature of the air on the secondary side ranges from 12-20 °C, the relative humidity of the air in the wet mode is maintained at 60%, and with the change in the outdoor temperature, the EER of the unit varies, as shown in Figure 13. When the dry-bulb temperature of the air on the secondary side is 12 ℃, the dry mode EER reaches up to 5.7, and as the temperature of the secondary-side air is gradually increased, the cooling capacity of the unit decreases, the input power remains unchanged, and the EER gradually decreases. At a dry-bulb temperature of the secondary-side air of 20 ℃, the EER decreases to 2.6. In the wet mode, with the secondary-side air RH maintained at 60% and a dry-bulb temperature of 12 ℃, the EER is 5.7. The EER decreases to 3 when the dry-bulb temperature is increased to 20 ℃. When the dry-bulb temperature is increased to 20 °C, the EER decreases to 3. When the dry-bulb temperature of the air on the secondary side is ≤14 °C, the EER in the wet mode is higher than that in the dry mode, and the wet mode provides a better refrigeration performance than the dry mode. In areas with a sufficient water supply, when the outdoor air dry-bulb temperature is 10-14 ℃, the operating hours of the wet mode can be extended, and the input power of the fan on the secondary air side can be adjusted according to the air temperature on the primary air side to improve the energy efficiency of the unit.

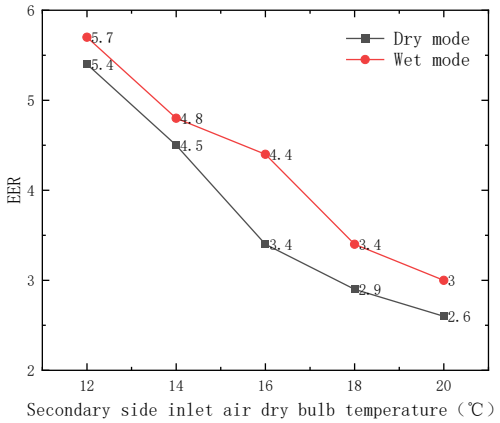

Figure. 13. EER changes of units at different temperatures

4. EXPLORATION OF THE REFRIGERANT CHARGE

The refrigerant charge is one of the important influencing factors of the heat transfer performance of a power separated heat pipe. An excessive liquid charge can result in incomplete liquid refrigerant vaporization in the evaporator, and gas–liquid mixtures can easily be formed in the pipeline between the evaporator and condenser, which affects the refrigerant transfer speed and causes the introduction of liquid refrigerant into the condenser, thus reducing the heat transfer efficiency of the condenser and the efficiency of the refrigerant cycle. A very high liquid charge can result in the tube wall of the evaporator not being fully covered by the liquid film, thus affecting the heat transfer efficiency. Therefore, determining the optimal refrigerant charge of refrigerant pump heat pipe systems is an important issue to ensure efficient heat transfer. In this experiment, three methods were selected to calculate the refrigerant charge.

4.1. Method 1

Wang (Wang Wen , Xiong Rui, Tu Chuan-jing, YEAR:1997 page 67-69) proposed a method for calculating the liquid charge of a separated heat pipe, considering the refrigerant charge of each component and connecting piping in the entire loop of the heat pipe.

① Liquid filling volume in the evaporation section

It is assumed that the dryness of the refrigerant mass linearly varies with filling volume; refer to Equation (4):

Equation 4:

$$M_1 = A_1 L_1 \frac{\ln(c_1 x - c_2 x + c_2) - \ln c_2}{x(c_1 - c_2)}$$

- $x =$ outlet dryness;
- $A_1 =$cross-sectional area of the evaporation section,(m^2);
- $L_1 =$length of the evaporation section, (m);
- $c_{1=}$ specific heat capacity of the saturated vapor, (kJ/(kg·K));
- $c_2 =$specific heat capacity of the saturated liquid, (kJ/(kg·K)).

② The intratracheal fluid filling volume can be obtained by Equation (5):

Equation5:

$$M_2 = \frac{A_2 L_2}{x_m c_1 + c_2 - x_m c_2}$$

- $A_2 =$ cross-sectional area of the vapor pipe, (m^2);
- $L_2 =$ length of the vapor tube, (m);
- $x_m =$ average dryness.

③ The condensing section charge can be determined by applying the Nusselt theory of condensation heat transfer, as expressed in Equation (6):

Equation6:

$$M_3 = 0.8\pi D_3 L_3 \left(\frac{4\mu\lambda}{g\rho^2 h_{fg}}\right)\left[\frac{qc}{0.943}\left(\frac{u_1 L_3}{g h_{fg}\rho^2\lambda^3}\right)^{1/3}\right]^{1/3}$$

- D_3 = diameter of the condensing section,(m);
- L_3 =length of the condensing section, (m);
- $\mu =$ dynamic viscosity of the saturated liquid, (Pa·s);
- λ = thermal conductivity of the saturated liquid, (W/(m^2·K));
- ρ =density of the saturated liquid, (kg/m^3);
- h_{fg} =latent heat of vaporization, (kJ/kg).

④ Fluid filling volume in the liquid tube; refer to Equation (7):

Equation7:

$$M_4 = A_4 L_4 \rho$$

- $A_4 =$cross-sectional area of the liquid tube, (m^2);
- $L_4 =$length of the liquid tube, m.

Consider the partial liquid charge at the time of heat pipe startup and regeneration and multiply the value by a factor of 1.05 for determining the overall liquid charge of the separated heat pipe; refer to Equation (8):

Equation8:

$$M = 1.05 \times (M_1 + M_2 + M_3 + M_4)$$

4.2. Method 2

Hong Zhang (Zhang Hong, YEAR:1996 page 13-17) proposed a method for calculating the refrigerant charge of a separated heat pipe, also considering the refrigerant charge in the evaporating section, the condensing end and the connecting piping, which can be expressed as follows:

① On the evaporation side, Equation (9) applies:

Equation9:

$$G_1 = \sum_{i=1}^{n} [\varepsilon_i \rho_v A + (1 - \varepsilon_i)\rho_l A]\delta z$$

- ε_i =gas content in the inner cross section of the pipe;
- ρ_v = density of gas-phase materials, (kg/m^3);
- A = pipe cross-sectional area, (m^2);
- ρ_l =liquid phase mass density, (kg/m^3);
- δ =liquid film thickness, (m);
- z = axial position, (m).

② The amount of vapor in the rising tube can be obtained by Equation (10):

Equation10:

$$G_2 = V_v^N A_s L_s \rho_v$$

- V_v^N = vapor phase fluid flow rate, (m/s);
- A_s =riser cross section, (m^2);
- L_s = riser tube length, (m).

③ On the condenser side, refer to Equation (11):

Equation11:

$$G_3 = \frac{4q_c}{7h_{fg}} {L_c}^2$$

- q_c =heat flow density in the condensing section, (W/ m^2);
- h_{fg} = latent heat of vaporization, (J/kg);
- L_c = length of the condenser section, (m).

④ The volume of liquid in the drop tube can be calculated by Equation (12):

Equation12:

$$G_4 = \rho_l A_x L_x$$

- A_x =drop tube cross-sectional area, (m^2);
- L_x =drop tube length, (m).

⑤ Volume of liquid missing on the evaporation side; refer to Equation (13):

Equation13:

$$G_5 = (L_h - Z_B)\pi {r_i}^2 \rho_l$$

- L_h =heating section pipe length, (m);
- Z_B =burnout location, (m);
- r_i =inside radius of the pipe, (m).

⑥ Fluid charge needed for heat pipe startup:

G_6 is generally set to 5%.

⑦ Separate heat pipe system charging volume; refer to Equation (14):

Equation14:

$$G = G_1 + G_2 + G_3 + G_4 + G_5 + G_6$$

4.3. Method 3

There is currently an empirical algorithm for calculating the refrigerant charge of vapor compression refrigeration systems, as expressed in Equation (15):

Equation15: $$M = (V_1 \times 75\% + V_2 \times 85\% + V_3 \times 15\% + V_4 + V_5 \times 15\%) \times \rho_l + V_6 \times \rho_g$$

- V_1 =volume of the evaporator, (m^3);
- V_2 =volume of the reservoir, (m^3);
- V_3 = volume of the gas–liquid separator, (m^3);
- V_4 =volume of the tube, (m^3);
- V_5 = volume of the condenser, (m^3);
- V_6 =tracheal volume, (m^3);
- ρ_l =density of the saturated liquid refrigerant at the evaporating temperature, (kg/m^3);
- ρ_g =density of the saturated gaseous refrigerant at the condensing temperature, (kg/m^3).

The refrigerant charge of the refrigerant pump heat pipe system was calculated using this method, and the results are shown in Table 4.

Table 4: Refrigerant charge of each component

Component	Volume (m^3)	Refrigerant charge (kg)
evaporator	0.0123	11.07
condenser	0.0167	3.01
reservoir	0.0135	13.77
gas–liquid separator	0.0106	1.908
liquid lines	0.000147	0.18
gas lines	0.000161	0.0066

These three methods consider the refrigerant charge of each component of the entire separated heat pipe system, but in regard to the evaporative condensation refrigerant pump heat pipe unit in this experiment, since the refrigerant pump is used to provide power for the whole separated heat pipe system, the liquid reservoir is an important component to ensure the normal operation of the refrigerant pump. Notably, Methods 1 and 2 lack the consideration of the refrigerant quantity in the liquid reservoir. The final refrigerant charge obtained by the three methods is as follows: Method 1: 34.65 kg; Method 2: 33.59 kg; and Method 3: 29.94 kg.

To study the influence of the different charging amounts on the heat transfer performance of the refrigerant pump heat pipe system, the charging amount is adjusted from 28-36 kg, and the unit is operated in the dry mode, thereby assessing the cooling capacity of the unit and the primary side air outlet temperature, and the results are shown in Figure 9. When the charging amount is 32 kg, the highest cooling capacity of the unit is 112.1 kW and the lowest primary air outlet temperature is 22.3 ℃, which shows that the optimal refrigerant charging amount of the refrigerant pump heat pipe system of this unit is 32 kg.

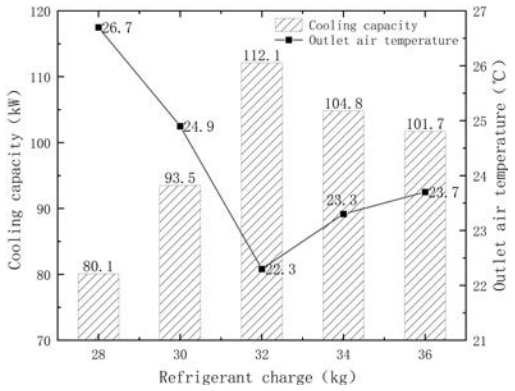

Figure. 14 Relationship between refrigerant charge, cooling capacity and outlet air temperature

In addition, the pressure difference between the inlet and outlet of the refrigerant pump decreases with decreasing refrigerant charge. Via the analysis, it is found that when the refrigerant charge is decreased, the liquid refrigerant in the reservoir decreases, so the refrigerant entering the refrigerant pump decreases, which leads to a lower mass flow rate of refrigerant in the refrigerant pump. Therefore, it is considered that there is still room for refrigerant charging in the reservoir. The refrigerant charge in the reservoir is increased from 85% to 100%, i.e., 2.43 kg of refrigerant is added, and the

refrigerant charge of the heat pipe system of the refrigerant pump is 32.37 kg, which is basically the same as the experimental result. Since the suction force of the refrigerant pump is lower than that of the compressor, the amount of refrigerant in the reservoir is more important, and if there is too much gaseous refrigerant in the reservoir, this could easily result in the refrigerant pump not being able to suction the liquid, and the refrigeration capacity of the heat pipe system of the refrigerant pump could be reduced.

Therefore, an improved simple algorithm for refrigerant charging is proposed, as expressed in Equation (16):

Equation16: $$M = (V_1 \times 75\% + V_2 + V_3 \times 15\% + V_4 + V_5 \times 15\%) \times \rho_l + V_6 \times \rho_g$$

- V_1 =volume of the evaporator, (m^3);
- V_2 =volume of the reservoir, (m^3);
- V_3 = volume of the gas–liquid separator, (m^3);
- V_4 =volume of the tube, (m^3);
- V_5 = volume of the condenser, (m^3);
- V_6 =tracheal volume, (m^3);
- ρ_l =density of the saturated liquid refrigerant at the evaporating temperature, (kg/m^3);
- ρ_g =density of the saturated gaseous refrigerant at the condensing temperature, (kg/m^3).

For the refrigerant pump heat pipe system, the refrigerant charge in the reservoir should not be neglected, and the refrigerant charge in the reservoir of this unit accounts for 50% of the total refrigerant charge of the system. The improved calculation method provides a novel idea for the calculation of the refrigerant charge of the refrigerant pump heat pipe system, the improved calculation method can be better applied in the new design of the unit or system modification.

5. CONCLUSIONS

In this paper, we describe the advantages of using a microchannel heat pipe evaporative condensation air-conditioning unit with a microchannel heat exchanger and evaporative condensation, we introduce the working principle of the unit as well as the three working modes, and we conduct experimental tests of the unit heat pipe system and mechanical refrigeration system. The following conclusions can be obtained:

(1) The maximum refrigeration capacity of the unit in the dry, wet and mixed modes is 112.1, 105.8 and 115.4 kW, respectively, and the primary-side air outlet temperatures are 22.3, 23.9 and 22.6 °C, respectively. The optimal air volume ratios are 2.2, 1.8 and 1.8, respectively. The energy efficiency of the unit is assessed, yielding the order of dry mode>wet mode>mixed mode, and the energy efficiency of the unit gradually decreases with increasing air volume ratio.

(2) As the outdoor dry- and wet-bulb temperatures increase, the cooling capacity of the unit gradually decreases. The dry-bulb temperature of the air on the secondary side impacts the cooling capacity in the dry mode, and the wet-bulb temperature of the air on the secondary side influences the cooling capacity in the wet mode. When the dry-bulb temperature of the air on the secondary side is 12~20 ℃, the EER in the wet mode is better than that in the dry mode, and in areas with a sufficient water supply, the duration of the wet mode can be extended at temperatures ranging from 10~14 ℃ to improve the energy efficiency of the unit.

(3) The optimal refrigerant charge of the refrigerant pump heat pipe system of the unit is 32 kg, at which time the cooling capacity of the unit is the highest, at 112.1 kW, and the primary-side air outlet temperature is the lowest, at 22.3℃, which is basically consistent with the value of 32.37 kg calculated by the proposed simple algorithm.

6. ACKNOWLEDGEMENT

The authors gratefully acknowledge the generous funding from Opening Funds of State Key Laboratory of Building Safety and Built Environment (BSBE-EET2024-04)

7. REFERENCES

[1] Insight 2021: Competitive Landscape and Market Share of China's Data Center Industry [J]. Data center construction+, 2021(8):4.

[2] Jiang L, Yong T, Wei Z, et al. Design and fabrication of sintered wick for miniature cylindrical heat pipe[J]. Transactions of Nonferrous Metals Society of China, 2014, 24(1): 292-301.

[3] Liu C，Chen Y，Feng D,et al. Experimental study on temperature uniformity and heat transfer performance of nitrogen loop heat pipe with large area and multi-heat source[J]. Applied thermal engineering: Design，processes，equipment，economics，2022(210-):210.

[4] Ma G Y，Wei C C，Zhang S，et al. Application of a pumped loop heat pipe heat exchanger unit for a small data center[J]. Beijing Gongye Daxue Xuebao / Journal of Beijing University of Technology，2015，41(3):439-445.

[5] A J D，A Y L，B S D，et al. Experimental investigation of an integrated cooling system driven by both liquid refrigerant pump and vapor compressor[J]. Energy and Buildings，2017，154:560-568.

[6] Yan G, Feng Y, Peng L. Experimental analysis of a novel cooling system driven by liquid refrigerant pump and vapor compressor[J]. International Journal of Refrigeration, 2015, 49: 11-18.

[7] Shuailing L, Guoyuan M, Xiaoya J, et al. Performance of a mechanically-driven loop heat pipe heat recovery system[J]. Applied Thermal Engineering, 2022, 207: 118066.

[8] Chen F, Zhou X, Liao S. Energy Saving Model and Calculation Example of Three Cooling Schemes for Data Center in Hot Summer and Cold Winter Area[J]. Journal of Power and Energy Engineering, 2022, 9(12): 1-20.

[9] Shuailing L，Guoyuan M，Xiaoya J，et al. Performance of a mechanically-driven loop heat pipe heat recovery system[J].Applied thermal engineering: Design, processes，equipment，economics，2022(207-):207.

[10] Ohadi M M，Dessiatoun S V，Choo K，et al. A comparison analysis of air，liquid, and two-phase cooling of data centers[C]// 2012:58-63.

[11] Wei A，Ren X，Lin S，et al. CFD analysis on flow and heat transfer mechanism of a microchannel Ω-shape heat pipe under zero gravity condition[J].International Journal of Heat and Mass Transfer，2020，163:120448.

[12] Han Z , Xue D , Wei H , et al. Study on operation strategy of evaporative cooling composite air-conditioning system in data center[J]. Renewable Energy, 2021, 177.

[13] Yue zheng M , Shu xue X , Guo yuan M ,et al. Characteristic Analysis and Experimental Study on a Hybrid System with Magnetic Pump-driven Two Phase Cooling System[J].Journal of Refrigeration, 2016,37(03):1-5.

[14] Lin Yucong, Liu Jinping, Xu Xiongwen ,et al. Experimental Research on Air Conditioning System of a Computer Room Based on Refrigerant Pump Pressurization[J].Journal of Refrigeration, 2020,41(05):83-88.

[15] Xue Lianzheng, Ma Guoyuan, Zhou Feng, et al. Performance Analysis of Gas-Pump-Driven Free-cooling Unit in a Small Data Center[J].Journal of Refrigeration, 2019,40(04):1-9.

[16] Bai Kaiyang, Ma Guoyuan, Zhou Feng , et al. Performance characteristics of pump-driven mechanical refrigeration and thermosyphon integrated system[J]. Heating Ventilating & Air Conditioning,2016,46(09):109-115.

[17] Liu Zhenyu, Huang Xiang, Chang Jianpei , et al. Design and test analysis of evaporative cooling(condensation) air conditioning unit data center [J]. Refrigeration and Air-conditioning, 2020, 20(1):6. (in Chinese)

[18] GB 50174-2017. Code for design of data centers [S].Beijing: China planning press，2017.(in Chinese)

[19] T/DZJN 27—2021. Evaporative cooling air - conditioning equipment of data centers [S]. Beijing：China planning press，2021. (in Chinese)

[20] Wang Wen , Xiong Rui, Tu Chuan-jing．Analysis of the Filling Quantity for Separated Type Heat Pipe．Power Engineering ,1997(03):67-69+73. (in Chinese)

[21] Zhang Hong. Inverstigation on the optimized working status of separated type heat pipe heat exchangers [J]. Petrochemical Equipment Technology,1996(03):13-17+65. (in Chinese)